Published in final edited form as:
Science. 2018 March 09; 359(6380): 1143–1146. doi:10.1126/science.aao4960.

Local transformations of the hippocampal cognitive map

Julija Krupic[1,2,*], **Marius Bauza**[2,3], **Stephen Burton**[2,3], and **John O'Keefe**[2,3]

[1]Department of Physiology, Development and Neuroscience, University of Cambridge, Cambridge, CB2 3EG, UK

[2]Department of Cell and Developmental Biology, University College London, London WC1E 6BT, UK

[3]Sainsbury Wellcome Centre, University College London, London W1T 4JG, UK

Abstract

Grid cells are neurons active in multiple fields arranged in a hexagonal lattice and are thought to represent the "universal metric for space." However, they become nonhomogeneously distorted in polarized enclosures, which challenges this view. We found that local changes to the configuration of the enclosure induce individual grid fields to shift in a manner inversely related to their distance from the reconfigured boundary. The grid remained primarily anchored to the unchanged stable walls and showed a nonuniform rescaling. Shifts in simultaneously recorded colocalized grid fields were strongly correlated, which suggests that the readout of the animal's position might still be intact. Similar field shifts were also observed in place and boundary cells—albeit of greater magnitude and more pronounced closer to the reconfigured boundary—which suggests that there is no simple one-to-one relationship between these three different cell types.

Place (1), head-direction (2), boundary (3–5), and grid cells (6) constitute the major units of the hippocampal cognitive map that forms the basis of our ability to navigate and form episodic memories (7). Based on the grid cell periodic firing pattern and presumed invariance, the predominant hypothesis of grid cell function states that they represent the spatial metric system of the brain (8). According to the major computational models, place and border cells act predominantly to stabilize the grid without determining its hexagonality (9–12). However, it has been recently shown that boundaries can profoundly reshape grid cell symmetry (13, 14), but the nature of this influence, as well as its relation to other spatial cells, remains unknown.

To study the effect of boundaries on grid cell structure, we recorded from 347 spatially periodic cells (15) in the medial entorhinal cortex (seven rats) (fig. S1A). The firing pattern

[*]**Corresponding author.** jk727@cam.ac.uk.

Author contributions: J.K., M.B., and J.O'K. designed and implemented the study and wrote the manuscript. S.B., M.B. and J.K. performed the experiments. J.K. planned the analysis. J.K. and M.B. analyzed the data. All authors discussed the results and contributed to the manuscript.

Competing interests: The authors declare no competing financial interests.

Data and materials availability: All data and code is available at www.krupiclab.com.

Europe PMC Funders Author Manuscripts

of the majority (63%) exhibited hexagonal symmetry in at least one of our four enclosures (grid cells), whereas that of other cells was more elliptical and irregular or had too few fields and did not pass the hexagonality criterion (fig. S2). Recordings were made while rats foraged for food in four familiar polygonal enclosures (presented in random order) that varied in shape from a left trapezoid (poly 129°) to a rectangle (poly 180°), with two intermediate shapes being irregular pentagons created by increasing the angle of the west-slanting wall of the trapezoid from 129° to either 145° or 160° (Fig. 1A).

We found that individual grid fields close to the slanting wall underwent average shifts as large as 41.6 cm (the largest in the rectangle to poly 145° transformation), whereas distant fields remained largely unchanged [the minimum (0.6 cm) and median (3.3 cm) field shifts in the same rectangle to poly 145° transformation], suggesting that the grid was influenced by the moving wall segment while remaining primarily anchored to the stable east (or north) wall (Fig. 1 and fig. S3). Fields as far as 78 cm in the x direction from the slanting wall (Fig. 1C, top) shifted more than expected by chance (as measured in repeated trials in the same enclosure, 5.7 cm) (see the supplementary materials). The amount of shift was inversely correlated with the distance to the slanting wall ($\rho_x = 0.93$, $P < 10^{-5}$; $\rho_y = 0.88$, $P = 0.004$, linear regression) (Fig. 1C), whereas the direction of shift was predominantly vertical, horizontal, or perpendicular to the slanting wall (Fig. 1D). Four head direction cells (three rats) recorded during such transformations showed little systematic change (fig. S4). The grid deformation was present for as long as we could record [>39 days in the rat (R2405) with the longest grid cell recordings] (fig. S5).

We next looked for the mechanism that could explain such grid deformations. First, we confirmed that the field movements did not result from changes in the animal's behavior in different geometric enclosures (figs. S6 and S7). Next, we ruled out the appealing hypothesis that the local shifts reflected purely short-range deformations resulting from individual "noninteracting" grid fields maintaining fixed distances of 30 (the typical border cell width), 50, or 70 cm to the walls (fig. S8). Finally, we investigated whether the field shifts could result from a global change in grid scale with the offset fixed only to the stationary east (or north) wall (fig. S9). The average grid rescaling was significantly different in contracting versus expanding enclosures (–2.0 ± 1.1% and 5.5 ± 1.2%, respectively; $P = 5.5 \times 10^{-6}$; $t_{554} = 4.59$; two-sample t test) (Fig. 2, A and B). In most transformations, rescaling was nonuniform across the enclosure (Fig. 2, C to E and supplementary materials). Importantly, the maximum field shift did not significantly correlate with grid scale and was comparable across all the recorded grid modules (Fig. 3, A to C) ($\rho = 0.19$, $P = 0.72$, linear regression; six grid cell modules with scales ranging from 29 to 86 cm in five rats), indicating that the ratio of scales between neighboring grid modules is not constant [also see (16)]. Furthermore, simultaneously recorded grid cells from different—as well as the same—grid modules showed a significant correlation between the magnitudes and directions of colocalized field shifts (Fig. 3, C to D). This indicates that the animal's position can be accurately decoded after a compensation for grid transformation; in contrast, uncoupled grid transformations could not be compensated and would result in reduced accuracy (Fig. 3E, fig. S10). The decoding error is also more pronounced close to the slanting wall for the nonlinear grid transformation compared to the linear, with the reversed tendency close to the stable wall (Fig. 3F).

What could underlie this nonhomogeneous grid rescaling? Previously, we suggested that competing place cells might constitute the basic building blocks of grid cells (17). In this model, a shift in one place-field position influences the positions of adjacent place fields, with the interaction force steeply decreasing as a function of the distance between fields. To test this idea, we recorded from 382 CA1 place cells (six rats) (fig. S1B) in the same enclosures. Like grids, place fields in close proximity to the slanting wall shifted with the wall, whereas the rest remained largely unaffected (Fig. 4). However, overall maximum place-field shift was significantly larger than that of the comparable colocalized grid fields (average difference across all transformations: 2.8 ± 0.24 cm, $P = 10^{-27}$, $t_{722} = 11.6$, two-sample t test). The shifts between simultaneously recorded colocalized grid cells (53) and place cells (101) (59 transformations, three rats) (fig. S11) were not significantly correlated (magnitudes and directions: 0.12 ± 0.07 and 0.08 ± 0.07, respectively, 11 transformations; $P = 0.25$, binomial test), although in some cases the correlation showed a trend toward significance (fig. S11). This could indicate that some place cells may be in register with grid cells and others not, possibly related to different spatial influences, such as those from border cells.

We found that individual grid fields shift by different amounts in response to local changes in enclosure geometry and that the magnitude of the shift is inversely correlated with the distance from the movable wall. Importantly, the grid remains primarily anchored to the stable wall of the enclosure, consistent with previous studies on other spatial cells and behavior, showing that the extent of cue control depends on its perceived stability (18–20). These results suggest that the local geometry of the enclosure plays a key role in constructing the grid as indicated by previous behavioral observations that rats relied on local geometry to find a reward location (21, 22). We have also shown that colocalized grid fields remained in register across all grid cells, including ones from different grid modules, suggesting that in principle these distortions could be corrected by the readout system to estimate the metric (23). Perhaps more likely, the transformed grids could lead to a misperception of self-location in the room frame of reference.

Finally, we found that grid cells could undergo nonuniform transformations that might be implemented either by the Field-Boundary Interaction model (17) or by the Boundary Vector Cell model (24, 25). Place cells show similar tendencies, albeit overall they shift by larger amounts. Previously it has been shown that place cells can be formed even in the absence of grid cells (26). Here, we demonstrate that they can undergo a different degree of transformation in response to the same geometric manipulation, suggesting that some place cells may be interacting with grid cells while others interact with border cells, as previously suggested (27), or alternatively their spatial properties may be formed by different underlying mechanisms.

Supplementary Material

Refer to Web version on PubMed Central for supplementary material.

Acknowledgments

We thank E. Spokaite and D. Macikenas for helpful discussions and L. Kukovska for help with single-unit isolation.

Funding: The research was supported by grants from the Wellcome Trust grants 090843/C/09/Z, 090843/D/09/Z, and 100154/Z/12/A and the Gatsby Charitable Foundation grants GAT3212 and GAT3531. J.K. is a Wellcome Trust/Royal Society Sir Henry Dale Fellow (grant 206682/Z/17/Z) and is supported by Kavli Foundation Dream Team project RG93383 and Isaac Newton Trust 17.37(t). J.O'K. is a Wellcome Trust Principal Research Fellow grant 203020/Z/16/Z.

References

1. O'Keefe J, Dostrovsky J. Brain Res. 1971; 34:171–175. [PubMed: 5124915]
2. Taube JS, Muller RU, Ranck JB Jr. J Neurosci. 1990; 10:420–435. [PubMed: 2303851]
3. Solstad T, Boccara CN, Kropff E, Moser M-B, Moser EI. Science. 2008; 322:1865–1868. [PubMed: 19095945]
4. Lever C, Burton S, Jeewajee A, O'Keefe J, Burgess N. J Neurosci. 2009; 29:9771–9777. [PubMed: 19657030]
5. Savelli F, Yoganarasimha D, Knierim JJ. Hippocampus. 2008; 18:1270–1282. [PubMed: 19021262]
6. Hafting T, Fyhn M, Molden S, Moser M-B, Moser EI. Nature. 2005; 436:801–806. [PubMed: 15965463]
7. O'Keefe, J, Nadel, L. The Hippocampus as a Cognitive Map. Oxford Univ. Press; 1978.
8. Moser EI, Moser M-B. Hippocampus. 2008; 18:1142–1156. [PubMed: 19021254]
9. McNaughton BL, Battaglia FP, Jensen O, Moser EI, Moser M-B. Nat Rev Neurosci. 2006; 7:663–678. [PubMed: 16858394]
10. Fuhs MC, Touretzky DS. J Neurosci. 2006; 26:4266–4276. [PubMed: 16624947]
11. Burgess N, Barry C, O'Keefe J. Hippocampus. 2007; 17:801–812. [PubMed: 17598147]
12. Hasselmo ME. Hippocampus. 2008; 18:1213–1229. [PubMed: 19021258]
13. Krupic J, Bauza M, Burton S, Barry C, O'Keefe J. Nature. 2015; 518:232–235. [PubMed: 25673417]
14. Stensola T, Stensola H, Moser M-B, Moser EI. Nature. 2015; 518:207–212. [PubMed: 25673414]
15. Krupic J, Burgess N, O'Keefe J. Science. 2012; 337:853–857. [PubMed: 22904012]
16. Stensola H, et al. Nature. 2012; 492:72–78. [PubMed: 23222610]
17. Krupic J, Bauza M, Burton S, Lever C, O'Keefe J. Philos Trans R Soc Lond B Biol Sci. 2013; 369
18. Knierim JJ, Kudrimoti HS, McNaughton BL. J Neurosci. 1995; 15:1648–1659. [PubMed: 7891125]
19. Jeffery KJ. Neuropharmacology. 1998; 37:677–687. [PubMed: 9705005]
20. Biegler R, Morris RG. Q J Exp Psychol B. 1996; 49:307–345. [PubMed: 8962538]
21. Pearce JM, Good MA, Jones PM, McGregor A. J Exp Psychol Anim Behav Process. 2004; 30:135–147. [PubMed: 15078123]
22. Jones PM, Pearce JM, Davies VJ, Good MA, McGregor A. Behav Neurosci. 2007; 121:1258–1271. [PubMed: 18085879]
23. Stemmler M, Mathis A, Herz AVM. Sci Adv. 2015; 1
24. Barry C, et al. Rev Neurosci. 2006; 17:71–97. [PubMed: 16703944]
25. Keinath AT, Epstein RA, Balasubramanian V. bioRxiv. 2017 Dec 18.
26. Koenig J, Linder AN, Leutgeb JK, Leutgeb S. Science. 2011; 332:592–595. [PubMed: 21527713]
27. Brandon MP, Koenig J, Leutgeb JK, Leutgeb S. Neuron. 2014; 82:789–796. [PubMed: 24853939]

Europe PMC Funders Author Manuscripts

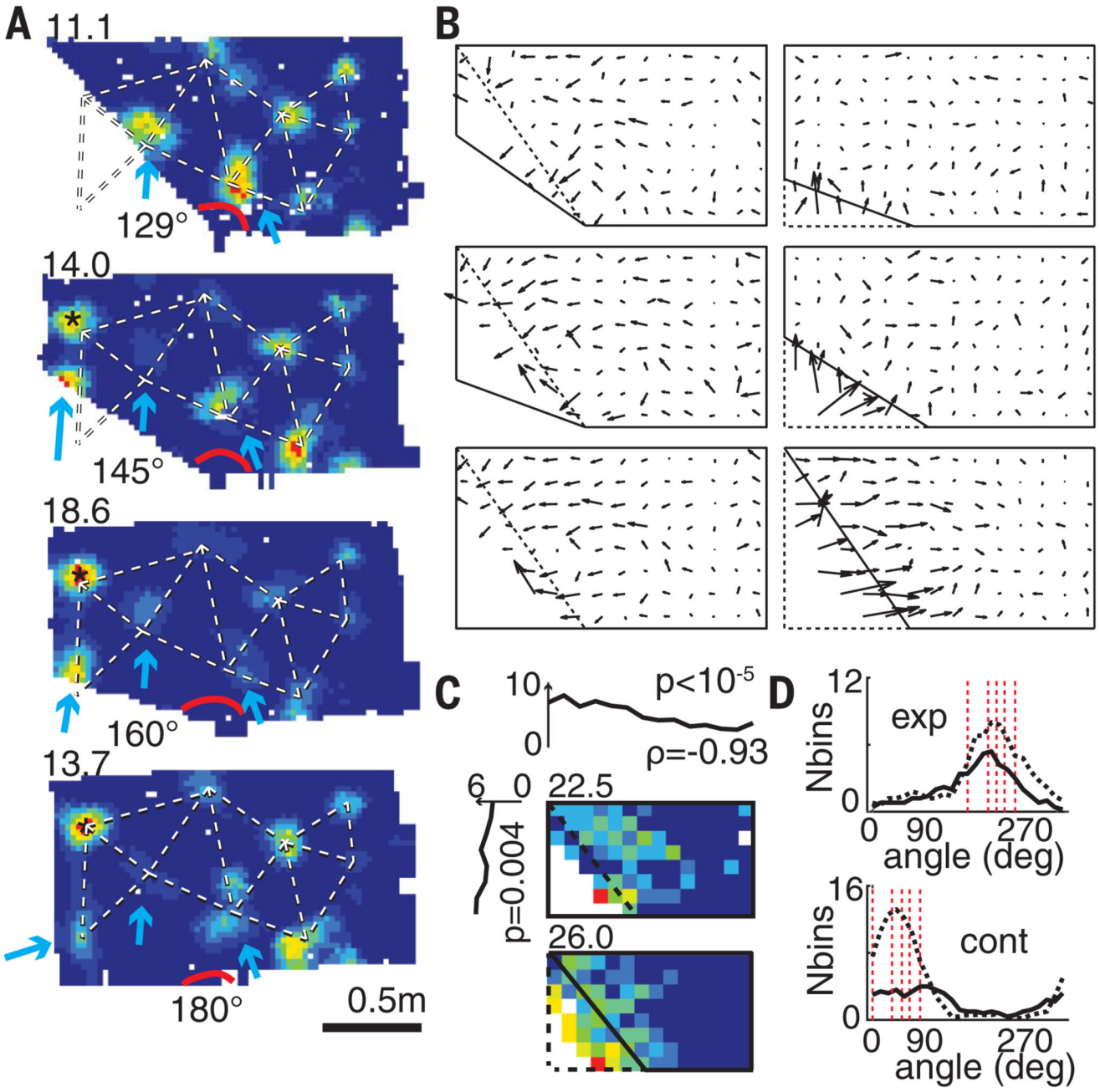

Fig. 1. Local grid deformations.

(**A**) A representative grid cell (R2338) where a single field adjacent to the slanting wall shifts, with lesser displacements in some farther fields and none in distant fields. (Top left) Peak firing rates. Blue arrows indicate moving fields, * indicates a newly emerged field, and red arc, the slanting angle. Dashed line outlines grid structure in the rectangle. (**B**) Mean vector fields of all the recorded grid cells indicating average field shifts between pairs of successive (but not necessarily immediately following each other) geometrical enclosures; the vector tail specifies field position in the first enclosure. The first and the second enclosures are shown in dashed and solid lines, respectively. (**C**) (Top and left) Mean field

shift across all transformations was inversely correlated with the distance to the slanting wall in x (top) and y (left) directions ($\rho_x = 0.93$, $P < 10^{-5}$; $\rho_y = 0.88$, $P = 0.004$); color-coded maps show the mean range of grid field shifts in poly 129° to rectangle (top) and rectangle to poly 129° transformations (bottom). (Top left) Peak shift in cm. (**D**) Directional changes of fields in expanding (exp) and contracting (cont) enclosures. (Top) Black solid and dashed lines represent transformations to poly 160° and rectangular enclosures, respectively. (Bottom) Black solid and dashed lines represent transformations to poly 129° and poly 145°, respectively. Dashed red lines show directions perpendicular to the slanting walls, as well as vertical and horizontal walls.

Europe PMC Funders Author Manuscripts

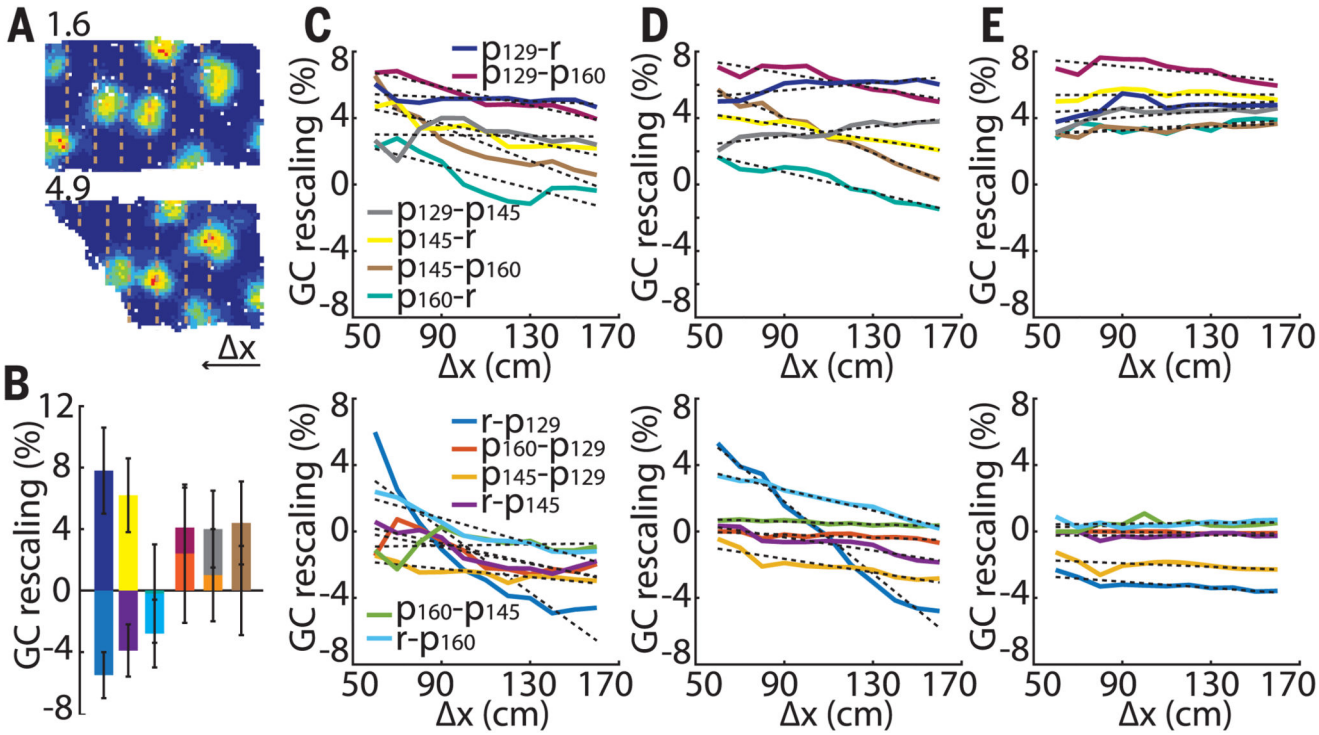

Fig. 2. Uniform versus nonuniform grid rescaling.

(**A**) A typical grid cell with larger changes close to the slanting wall. Dashed lines indicate matched successive increments from right to left in exposed areas for homogeneity analysis. (**B**) Average grid rescaling in different transformations. Different colors represent different transformations specified in (C). (**C**) Average grid rescaling in *x* direction. (**D** and **E**) Simulated grid rescaling with nonuniform (D) and uniform (E) grid rescaling.

Europe PMC Funders Author Manuscripts

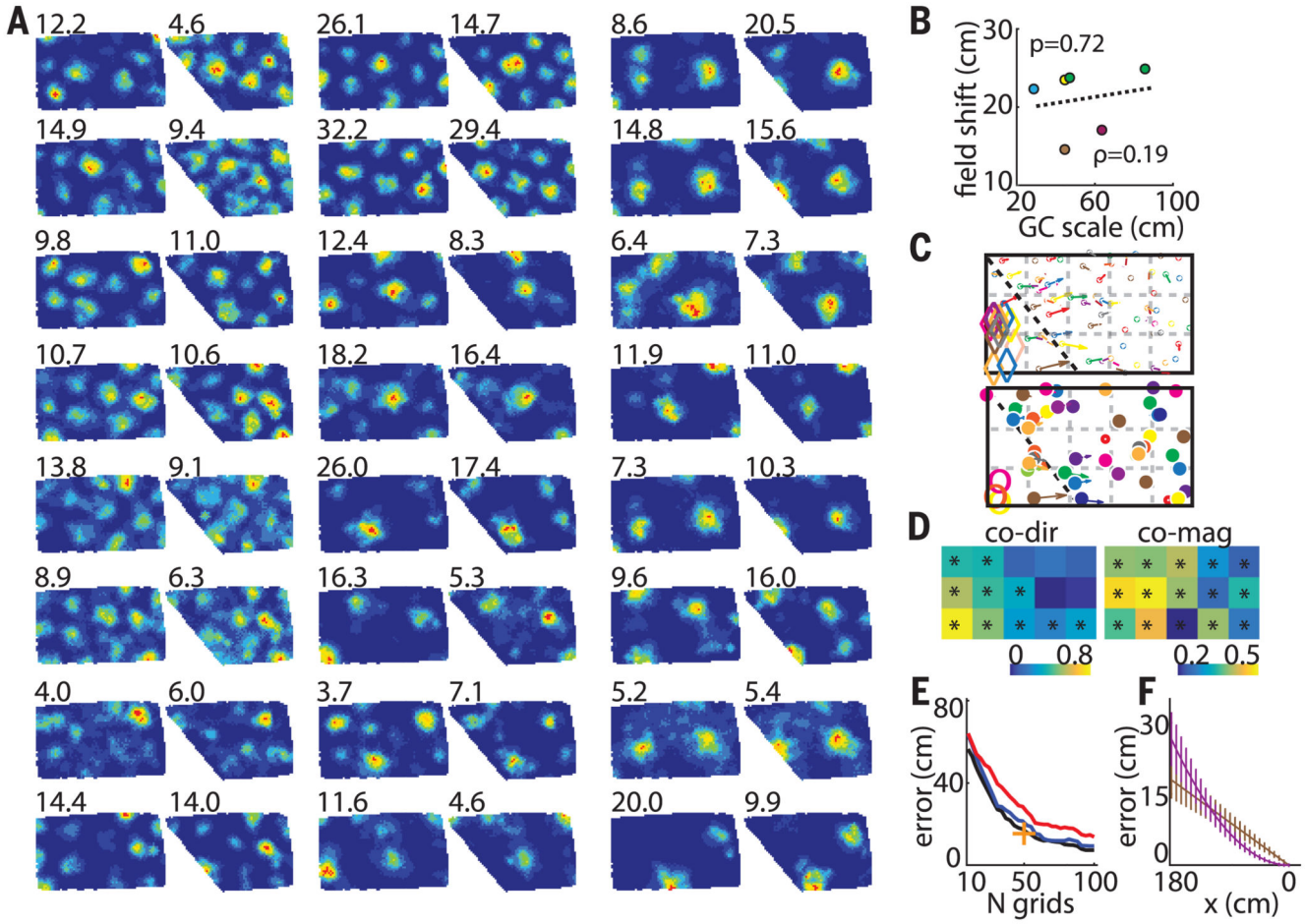

Fig. 3. Simultaneous changes in grid field positions.

(**A**) Twenty-four corecorded grid cells (R2405) from two different modules (ratio ~1.6). (Top left) Peak firing rate. (**B**) Maximum average field shifts versus grid scale of six different grid modules (five rats). Individual animals are shown with different colors (green, R2405). (**C**) Vector fields of cells in (A). (Top and bottom) Smaller and larger modules, respectively. Different colors correspond to different cells. Diamonds and open circles indicate fields that disappeared in poly 129°. (**D**) Similarity matrices of field shift directions (left) and magnitudes (right) between corecorded grid cells from five rats combined (R2405, R2383, R2338, R2375, and R2298). All transformations from poly 129° to a rectangle (and vice versa) and poly 145° to a rectangle (and vice versa) were included. GC-GC direction and magnitude similarity thresholds: 0.20 and 0.16, respectively. (**E**) Position decoding error decreases with the number of cells and is smaller in grids nonuniformly transformed in register (blue) compared with uncoupled ones (red). Black indicates decoding in the absence of any transformation; + indicates decoding accuracy of our largest data set (50 simultaneously recorded grid cells). (**F**) Systematic position decoding error is larger in nonuniformly (violet) compared with uniformly (brown) transformed grid cells close to the slanting wall. The tendency reverses close to the stable east wall.

Europe PMC Funders Author Manuscripts

Europe PMC Funders Author Manuscripts

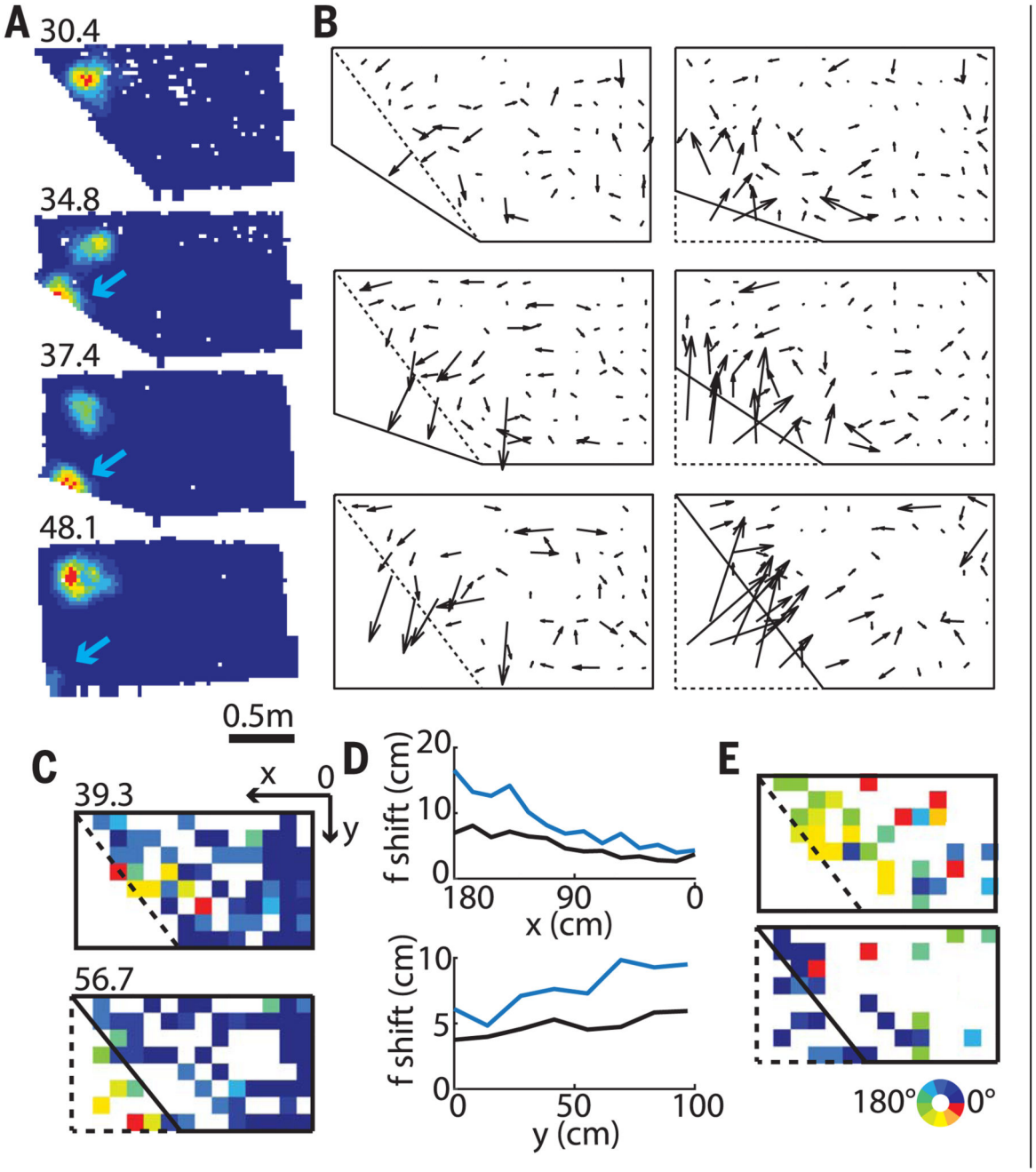

Fig. 4. Local changes in place fields.

(**A**) Representative place cell with one of its fields shifting with the slanting wall while a second more distant field remains stable. (Top left) Peak firing rate. (**B**) Mean vector fields indicating the average place-field shifts between successive pairs of different geometrical enclosures. (**C**) Color-coded map showing the range of vector magnitudes. First and second enclosures are shown in dashed and solid lines, respectively. (Top left) Peak shift in cm. (**D**) Mean field shifts in all transformations (place cells, blue; grid cells, black) in *x* (top) and *y* (bottom) directions were more pronounced in place cells compared to grid cells, with the

difference larger close to the slanting wall. (**E**) Color-coded map showing the range of vector directions.

Europe PMC Funders Author Manuscripts